European Polymer Journal 108 (2018) 286–294

Contents lists available at ScienceDirect

European Polymer Journal

journal homepage: www.elsevier.com/locate/europolj

Mechanistic study on the hydrolytic degradation of polyphosphates

Kristin N. Bauer, Lei Liu, Manfred Wagner, Denis Andrienko, Frederik R. Wurm*

Max Planck Institute for Polymer Research, Ackermannweg 10, 55128 Mainz, Germany

A B S T R A C T

Ring-opening polymerization of cyclic phosphates offers a fast access to well-defined, water soluble and (bio)degradable polyphosphoesters (PPEs). In particular, poly (alkyl ethylene phosphate)s have been used as building blocks for nanocarriers or hydrogels. The molecular mechanism of their degradation is, however, not well understood. Herein, we study the hydrolytic degradation of two most frequently used PPEs, poly(methyl ethylene phosphate) (PMEP) and poly(ethyl ethylene phosphate) (PEEP). The degradation process is analyzed by NMR spectroscopy, which identifies and quantifies intermediates and degradation product(s). We prove that the major degradation pathway is backbiting, leading to one dominating hydrolysis product, ethyl or methyl ethylene phosphate (a diphosphate). Accelerated hydrolysis, performed in basic and acidic conditions, shows the high stability of PEEs under acidic conditions, while they readily degrade under basic conditions. The backbiting mechanism is further supported by the reduction of the degradation kinetics if the terminal OH-group is blocked by a urethane. Our findings help to develop degradable nanodevices with adjustable hydrolysis kinetics.

1. Introduction

Biodegradable polymers are interesting materials for applications ranging from materials science to biomedicine [1,2]. They are especially appealing for temporary therapeutic applications [3], e.g. for the design of surgical implants or drug delivery vehicles [4,5]. They remain inside of the body only temporarily but eventually are biodegraded. This degradation can happen either by hydrolytic or enzymatic degradation or a combination of both [6,7]. The majority of biodegradable polymers is based on synthetic polyesters or modified biopolymers that are susceptible to enzymatic and/or hydrolytic cleavage [8]. The pre-evaluation of enzymatic degradation *in vivo* is difficult, due to varying enzyme concentrations at different sites in the body and often *ex vivo* investigations with purified enzymes or accelerated hydrolysis conditions are conducted [9]. For a few years, polyphosphoesters (PPEs), e.g. polyesters based on phosphoric acid, have been considered as promising degradable materials for diverse biomedical applications [10,11]. Synthetic PPEs are inspired from natural PPEs, such as DNA and RNA or teichoic acids. The biodegradation of these biopolymers has been studied in detail [12–14]. In contrast, for synthetic PPEs, the potential biodegradability and biocompatibility are emphasized in most publications about PPEs, but only a few detailed studies of their degradation mechanism are available [15,16]. PPEs are, however, very interesting candidates for bioapplication due to their potential polyfunctionality and adjustable degradation kinetics [17]. For example, the enzymatic degradation of polyphosphates was reported to occur by phosphatases [18,19]. Also poly(alkyl ethylene phosphonate)s – with a stable P-C-bond as a pendant group- have been reported to undergo much faster hydrolysis than the respective polyphosphates [20]. First studies on the kinetics of PPE hydrolysis were presented by Penczek in the 1990s [21]. They evaluated the hydrolysis of poly(methyl ethylene phosphate) (PMEP) at pH-values ranging from 2 to 12 and suggested two different mechanisms for hydrolysis under basic and acidic conditions. Under basic conditions, they proposed a direct nucleophilic attack of the OH^- ion on the phosphorus atom leading to an intermediate five-binding phosphorus with a trigonal bipyramidal geometry in which the axial position is preferably shed. Due to comparable probabilities for the main and side chains to occupy this position, these chains should be cleaved with the probability proportional to the Boltzmann prefactor. Under acidic conditions, however, they proposed a nucleophilic attack of H_2O on the α-carbon, after protonation.

Herein, we systematically investigated the hydrolysis of two poly (alkyl ethylene phosphate)s (with alkyl = methyl or ethyl, i.e. PMEP and PEEP), the two most frequently used and water-soluble PPEs. They are prepared by the ring-opening polymerization of the respective 5-membered cyclic phosphate monomers and are accessible in high control over molecular weight, dispersity, and end-group chemistries [10,22]. We propose a different hydrolysis mechanism, mainly happening from the chain end by a backbiting reaction, leading to a single degradation product, namely alkyl (2-hydroxyethyl) phosphate. This mechanism is supported by the characterization of the degradation product and by a drastic slowdown of the degradation kinetics if the OH-chain end is blocked by a stable urethane linkage. This is the first report on the detailed back-biting degradation of poly(alkyl ethylene phosphate)s and will be helpful for the design of future degradable polymer architectures based on PPEs.

* Corresponding author.
E-mail address: wurm@mpip-mainz.mpg.de (F.R. Wurm).

https://doi.org/10.1016/j.eurpolymj.2018.08.058
Received 16 July 2018; Received in revised form 28 August 2018; Accepted 31 August 2018
Available online 08 September 2018
0014-3057/

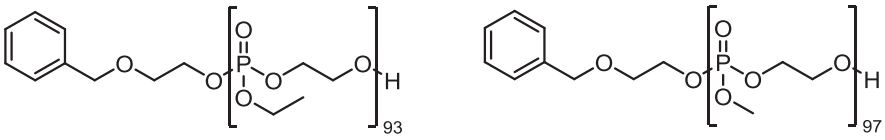

poly(ethyl ethylene phosphate)
(**PEEP**)

poly(methyl ethylene phosphate)
(**PMEP**)

Fig. 1. Chemical structures of the polyphosphates used in this study.

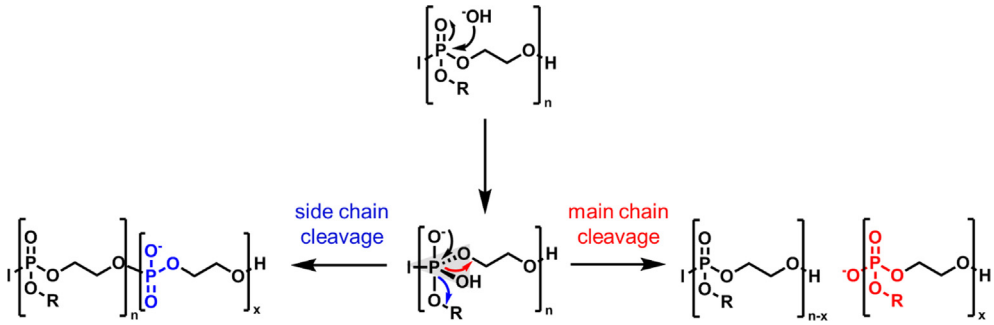

Scheme 1. Hydrolytic degradation of poly(alkyl ethylene phosphate)s (typically prepared by ring-opening polymerization of cyclic phosphoester) under basic conditions as reported in previous literature [21].

2. Experimental

2.1. General

All reagents were used without further purification unless otherwise stated. Solvents, dry solvents and deuterated solvents were purchased from Acros Organics, Sigma-Aldrich, Deutero GmbH or Fluka. 1,8-diazabicyclo[5.4.0]undec-7-ene was distilled prior to use, and stored over molecular sieve at 4 °C.

2.2. Methods

2.2.1. Size exclusion chromatography (SEC)

SEC measurements were conducted in DMF (containing 0.25 g L^{-1} of lithium bromide) at 60 °C on an Agilent 1100 Series as an integrated instrument, including a PSS GRAM columns (1000/1000/100 g), a UV detector (270 nm), and a RI detector at a flow rate of 1 mL min^{-1} at 60 °C. Calibration was carried out using PEO standards provided by Polymer Standards Service.

2.2.2. Nuclear magnetic resonance (NMR)

For nuclear magnetic resonance analysis ^{1}H, ^{13}C, and ^{31}P NMR spectra were recorded on a Bruker AVANCE III 300 or 500 MHz spectrometer. All polymer spectra were measured in either CDCl3 or CD_2Cl_2 and the spectra were calibrated against the solvent signal and analyzed using MestReNova 8 from Mestrelab Research S.L.

Degradation studies were recorded on a Bruker AVANCE III 500 MHz spectrometer. All degradation studies were conducted in H_2O containing 10% of D_2O.

To measure diffusion coefficient of ^{31}P-nuclei an INEPT based 2D measurement were used with non-selective polarisation transfer between protons and phosphorous nuclei using bipolar gradient pulses for diffusion.

In this work, the gradient strength was varied in 32 steps from 2% to 100%. The diffusion time was optimized at 50 ms and the gradient length to 1.4 ms. The chosen relaxation delay was set to 2 s.

2.2.3. DFT calculations

The structures were optimized at the B3LYP level of theory [23], in conjugation with the basis set of 6-311 + + G** [24]. The SMD solvation model was used to compute the solvation Gibbs free energies by employing water as the solvent [25]. All DFT calculations were carried out by means of Gaussian 09 package [26].

2.3. Synthetic procedures

2.3.1. Synthesis of poly(methyl ethylene phosphate) ($PMEP_{97}$)

All Schlenk-tubes were flame-dried prior to use. 2-(benzyloxy) ethanol was used as initiator and 1,8-diazabicyclo[5.4.0]undec-7-ene DBU (DBU)/1-(3,5-bis(trifluoromethyl)phenyl)-3-cyclohexylthiourea (TU) as catalyst/co-catalyst system. TU (121 mg, 328 µmol, 5 eq) was introduced into a flame-dried Schlenk-tube, dissolved in benzene, and dried by lyophilization. MEP (894 mg, 6.5 mmol, 100 eq) was added. 0.49 mL (9.9 mg, 64.8 µmol, 1 eq) of initiator stock solution (c = 20 mg mL^{-1} in dry DCM) was added and the monomer concentration was adjusted to 3 mol L^{-1}. The reaction mixture was cooled down to 0 °C and the polymerization was started by rapid addition of DBU (50 mg, 328 µmol, 5 eq). The polymerization was quenched after 1.4 h by addition of 2 mL of acetic acid in DCM (c = 20 mg mL^{-1}). The polymer was obtained as a colorless viscous liquid (819 mg, 92%) and purified by precipitation into diethyl ether and subsequent dialysis against water.

^{1}H NMR (300 MHz, Methylene Chloride-d_2) δ 7.33 (m, 5H), 4.54 (s, 2H), 4.51–4.02 (m, 378H), 3.78 (dd, J = 11.2, 5.9 Hz, 291H). ^{31}P NMR (121 MHz, Methylene Chloride-d_2) δ 1.04, −0.18, −1.42.

2.3.2. Synthesis of poly(methyl ethylene phosphate) ($PEEP_{93}$)

All Schlenk-tubes were flame-dried prior to use. 2-(benzyloxy) ethanol was used as initiator and DBU/TU as catalyst/co-catalyst system. TU (121 mg, 328 µmol, 5 eq) was introduced into a flame-dried Schlenk-tube, dissolved in benzene and dried by lyophilization. EEP (1026 mg, 6.7 mmol, 100 eq) was added to dissolve the TU co-catalyst. 0.51 mL (10.3 mg, 67.5 µmol, 1 eq) of initiator stock solution (c = 20 mg mL^{-1} in dry DCM) was added and the monomer concentration was adjusted to 3 mol L^{-1}. The reaction mixture was cooled down to 0 °C and the polymerization was started by rapid addition of DBU (50.0 mg, 328 µmol, 5 eq). The polymerization was quenched after 1.4 h by addition of 2 mL of acetic acid in DCM (c = 20 mg mL^{-1}). The polymer was obtained as a colorless viscous liquid (921 mg, 89%) and purified by precipitation into diethyl ether and subsequent dialysis against water.

^{1}H NMR (300 MHz, Methylene Chloride-d_2) δ 7.53–6.97 (m, 5H),

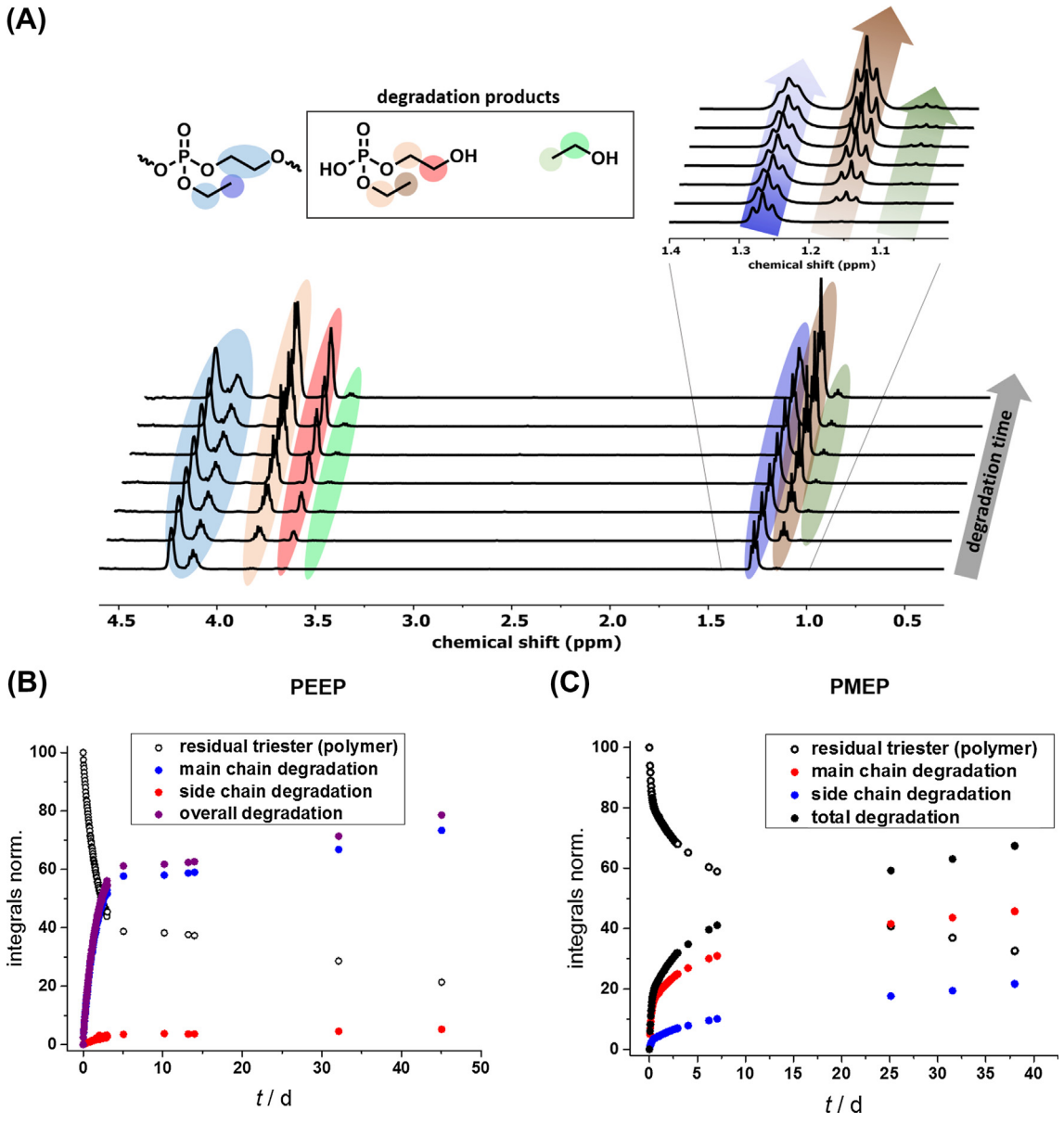

Fig. 2. (A) Overlay of several ^{1}H NMR spectra, which were recorded within the degradation process of $PEEP_{93}$. (B) and (C) degradation profiles of $PEEP_{93}$ and $PMEP_{97}$ at pH 11 derived from ^{1}H NMR spectra recorded throughout the degradation process.

4.47 (s, 2H), 4.43–3.82 (m, 546H), 3.66 (m, 2H), 3.63–3.57 (m, 2H), 1.26 (t, J = 7.1 Hz, 280H). ^{31}P NMR (121 MHz, Methylene Chloride-d_2) δ −1.29.

2.3.3. Synthesis of end-functionalized PEEP ($blPEEP_{89}$)

All Schlenk-tubes were flame-dried prior to use. 2-(benzyloxy) ethanol was used as initiator and DBU/TU as catalyst/co-catalyst system. TU (121 mg, 328 µmol) was introduced into a flame-dried Schlenk-tube, dissolved in benzene and dried by lyophilization. EEP (934 mg, 6.14 mmol, 100 eq) was added to dissolve the TU co-catalyst. 0.47 mL (9.4 mg, 61.4 µmol, 1 eq) of initiator stock solution (c = 20 mg mL^{-1} in dry DCM) was added and the monomer concentration was adjusted to 3 mol L^{-1}. The reaction mixture was cooled down to 0 °C and the polymerization was started by rapid addition of DBU (50.0 mg, 328 µmol). The polymerization was quenched after 1.25 h by rapid addition of ethyl isocyanate (93.41 mg, 1.31 mmol, 21 eq) at 0 °C. Subsequently, the cooling was removed and the reaction mixture was stirred for further 20 min. After removal of the solvent, the polymer was dissolved in THF:H_2O (1:1) and dialyzed against water twice. The polymer was obtained as a colorless viscous liquid (112 mg, 12% (due to product loss during purification)).

^{1}H NMR (300 MHz, Methylene Chloride-d_2) δ 8.01 (s, 1H), 7.48–7.23 (m, 5H), 4.52 (s, 2H), 4.46–3.80 (m, 510H), 3.72–3.66 (m, 3H), 3.20–3.12 (m, 3H), 1.34 (t, J = 7.1 Hz, 267H), 1.13 (m, 10H). ^{31}P NMR (121 MHz, Methylene Chloride-d_2) δ −1.30.

2.3.4. Buffer preparation

40 mL of Buffer solution with pH 11 were prepared by adding 20 mL of 0.4 M $NaHCO_3$-solution with 7.4 mL of 1 M NaOH solution and 8.6 mL H_2O and 4 mL D_2O to achieve a H_2O:D_2O ratio of 9:1. The pH of the buffer was determined with a pH electrode.

2.3.5. Degradation studies by NMR spectroscopy

For the NMR spectroscopic degradation studies of PEEP and PMEP 3.5 mg of polymer were dissolved in 0.75 mL of buffer solution. Degradation of the first 24–72 h was continuously followed by iterating ^{1}H and ^{31}P NMR spectroscopy. Subsequently, the intervals between the NMR spectra were increased.

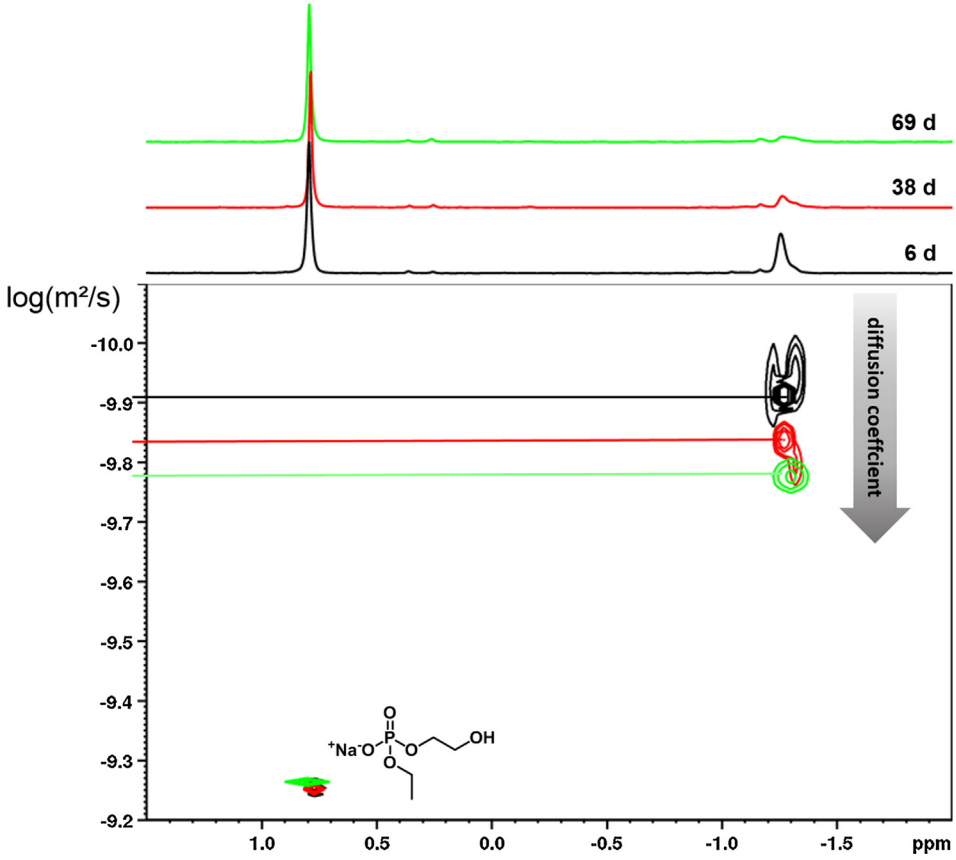

Fig. 3. ^{31}P DOSY NMR spectra (202 MHz, 298 K, H_2O/D_2O 9:1) recorded at different time points within the degradation process of $PEEP_{93}$.

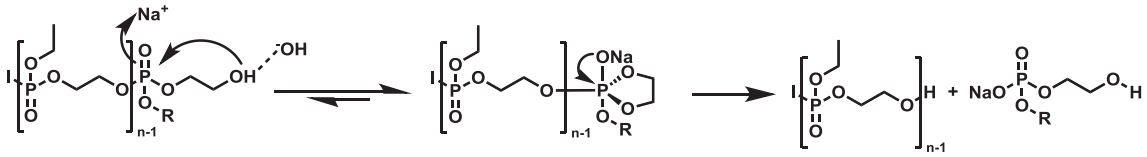

Scheme 2. Suggested degradation mechanism for the degradation of polyphosphates.

2.3.6. Degradation studies under acidic conditions

For the degradation of PEEP under acidic conditions, 3.5 mg of polymer were dissolved in 0.75 mL of 1 M HCl containing 10% of D_2O. The sample was stored at ambient temperature and NMR spectra were recorded at different time points.

2.3.7. Degradation studies by SEC analysis

For the degradation studies by SEC analysis, 3.5 mg of polymer were dissolved in 0.75 mL of buffer solution per Eppendorf vial. The samples were stored at room temperature until analysis. For SEC analysis, the vials were freezed with liquid nitrogen and dried by lyophilization. Subsequently, the residue was dissolved in DMF and analyzed by SEC.

3. Results & discussion

The hydrolytic degradation of poly(alkyl ethylene phosphate)s was investigated with regard to the degradation mechanism, kinetics, and products. Two hydrophilic PPEs with similar degree of polymerization were analyzed: poly(ethyl ethylene phosphate) (PEEP, M_n = 14,300 g/mol (from NMR), $Đ$ = 1.10 (from SEC)) and poly(methyl ethylene phosphate) (PMEP, M_n = 13,500 g/mol (from NMR), $Đ$ = 1.52 (from SEC), Fig. 1). These two PPEs were prepared by ring-opening polymerization of the respective phospholane monomers and have been used in various previous studies as water-soluble segments in nanoassemblies and nanocarriers, mainly as a substitute for the non-biodegradable poly(ethylene glycol) [27–29].

Detailed investigation on the accelerated hydrolysis of the PPEs was conducted under both acidic (at pH = 0 (1 M HCl)) and basic conditions (pH = 11 in a $NaHCO_3$/NaOH buffer). The degradation was followed by SEC, ^{1}H, and ^{31}P NMR spectroscopy, allowing identification of degradation mechanism and products. PPEs can be degraded by the hydrolytic cleavage of the three ester linkages. Under aqueous basic conditions, degradation had been reported to happen by nucleophilic attack of the hydroxyl ions on any central phosphorus atom of the repeating units [21]. The ester cleavage can happen either in the polymer main or side chain, whereas only the cleavage of ester linkages in the main chain leads to polymer degradation. Instead, ester cleavage in the side chain leads to the formation of a polyphosphodiester, i.e. polyanions (Scheme 1). A further degradation of the resulting diesters is unlikely, due to the negative charge of the degradation product, hindering further nucleophilic attack of hydroxyl anions [30]. The formation of polyanions would also influence the performance of such polymers in bioapplications, as protein or cell interactions would be affected.

For PEEP and PMEP, the ester cleavage had been reported to occur at a random repeat unit within the polymer chain, whereas the cleavage of both side- and main-chain was expected to occur statistically with a ratio of 1:2 [21]. A differentiation between main and side chain ester

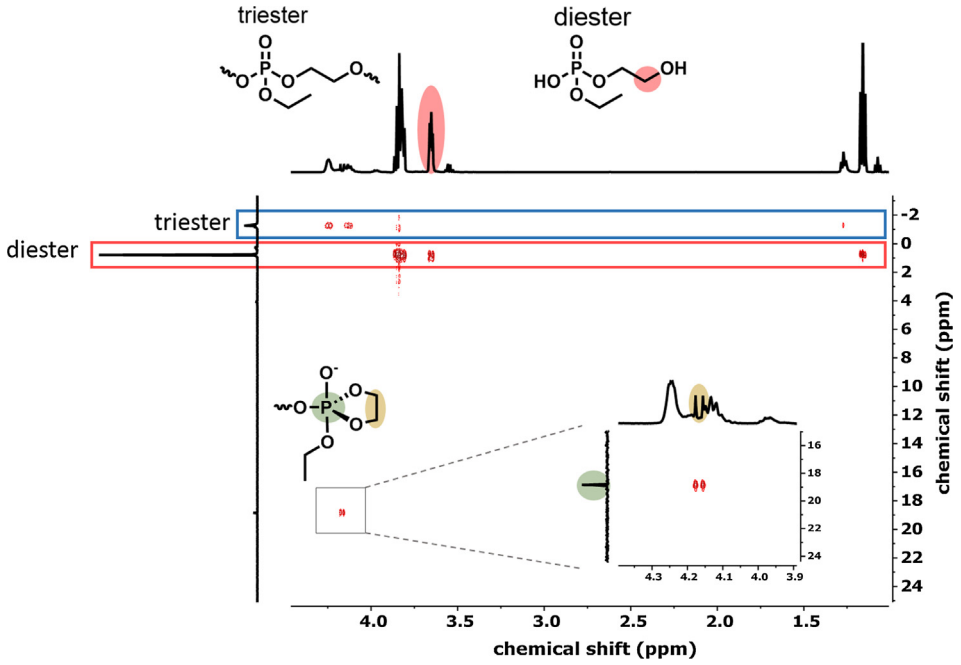

Fig. 4. ^{1}H, ^{31}P HMBC (500, 202 MHz, 298 K, H_2O/D_2O (9:1)) recorded within the degradation process of PEEP at pH 11.

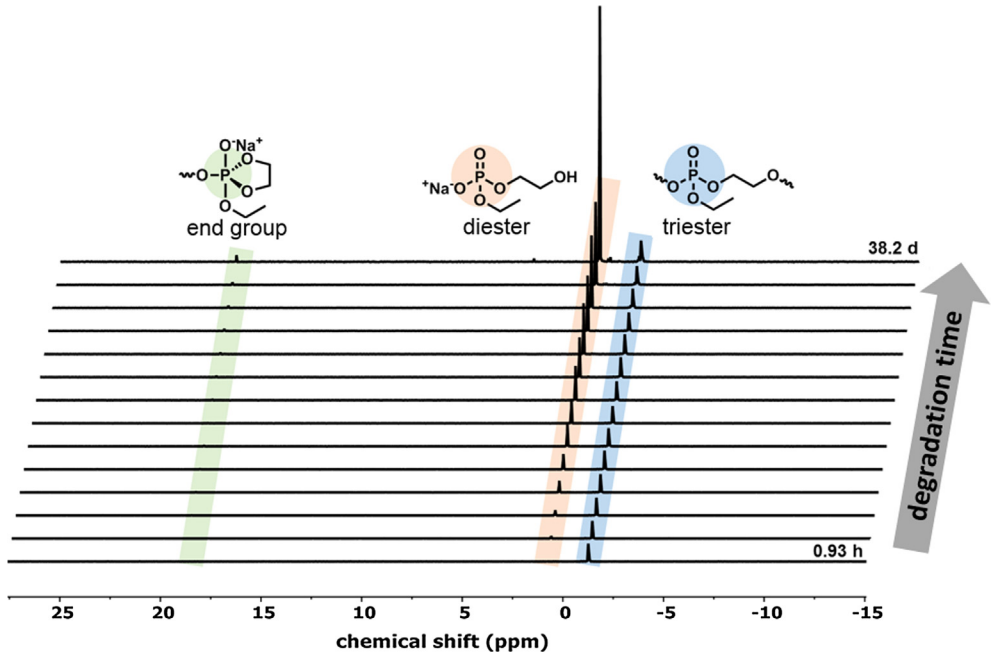

Fig. 5. ^{31}P NMR spectra (202 MHz, 298 K, H_2O/D_2O (9:1)) recorded within the degradation of $PEEP_{93}$ at pH 11.

cleavage can be derived from the recorded ^{1}H NMR spectra. Upon side chain cleavage ethanol or methanol are released, respectively, which can be identified by ^{1}H NMR spectroscopy. This cleavage pattern was also proven by our group recently for PPEs prepared by acyclic diene metathesis polymerization, which have longer alkyl chains between the phosphates, i.e. poly(alkyl alkylene phosphate)s [31]. For PPEs prepared by ring-opening polymerization of phospholanes, the CH_2-CH_2-segment is located between the phosphates and the polymer chain end carries a CH_2-CH_2-OH group, which distinctively change the degradation pathway as shown below. For PEEP, cleavage of the main-chain can be identified in the ^{1}H NMR spectra by the terminal methyl groups located in the pendant esters (i.e. the side-chains), which shift to the high field upon ester cleavage. In Fig. 2(A), an overlay of several ^{1}H NMR spectra are shown exemplarily, which were recorded within the degradation process of $PEEP_{93}$. In the region between 1.3 and 1.0 ppm three triplets can be detected, which correspond to the different degradation products and were used to quantify the degradation process. The triplet at 1.27 ppm can be attributed to the methyl group in the pendant chain of the intact triester (i.e. the PEEP-polymer as prepared) and was used to quantify residual polymer. The triplet at 1.07 can be assigned to the methyl group of ethanol released upon side chain cleavage. Thus, this signal was used for the quantification of side chain cleavage – it can be directly appreciated that the intensity for ethanol remains very low throughout the degradation time (in a closed setup). The adjacent triplet at 1.16 ppm can be attributed to the methyl group in the pendant chain of the diester formed upon ester cleavage in the

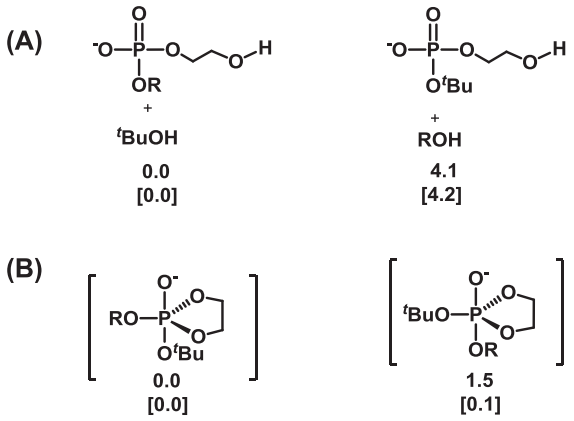

Fig. 6. DFT (B3LYP/6-311 + +G**, SMD (water)) calculated Gibbs free energies for the chain cleavage products (a), and the intermediate states (b). The values without and with bracket are for the R = Me, Et. All values are given in kcal mol^{-1}.

polymer backbone and was used for the quantification of main chain cleavage. Quantification of the degradation process of $PMEP_{97}$ was conducted analogously (NMR spectra can be found in the Supp. Info). Fig. 3 shows the degradation profile of $PEEP_{93}$ and $PMEP_{97}$ derived from ^1H NMR spectra at pH = 11. Both polymers showed a similar degradation profile with an initial rapid degradation phase which slows down in the second phase. However, the considered polymers showed significantly different behavior concerning the ratio of main and side chain cleavage. While within the degradation of $PMEP_{97}$ the expected ratio of 2:1 main and side chain cleavage was approximated after 40 days at pH = 11, the degradation of $PEEP_{93}$ is dominated by main chain cleavage. The predominant main chain cleavage of $PEEP_{93}$ might be attributed to increased steric hindrance in the side chain compared to $PMEP_{97}$. However, in contrast to PEEP with narrow molecular weight distributions, PMEP typically has broader distributions (Fig. S7). This was rationalized to enhanced transesterification during the polymerization process, which leads to branching of the polymer [32]. Branching points within the polymer structure lead to more complex degradation pattern, which can be seen in the ^{31}P NMR spectra recorded within the degradation of PMEP at pH 11 (Fig. S17).

For PEEP the dominant main chain cleavage indicated an alternative degradation mechanism preventing a statistical degradation of main and side chain. For polylactide (PLA), degradation was reported to occur by intramolecular transesterfication, so-called “backbiting”, initiated by the terminal hydroxyl function [33]. Hydroxyl ions catalyze the nucleophilic attack of the terminal hydroxyl function on the penultimate carbonyl group resulting in the formation of a terminal six-membered cycle, which is subsequently released and hydrolyzed to lactic acid. A similar mechanism is also conceivable for the degradation of polyphosphates (Scheme 2).

By backbiting of the terminal hydroxyl group a five-membered cycle is formed, in which either the side or the main chain can be cleaved. Upon main chain cleavage, one repeating unit is released and a polymeric product with n-1 repeating units remains. Thus, degradation by backbiting-mechanism is indicated by (i) the formation of one dominant degradation product, namely the sodium salt of ethyl (2-hydroxyethyl) phosphate or methyl (2-hydroxyethyl) phosphate respectively and (ii) the formation of a five-membered cycle at the polymer chain end. Furthermore, the backbiting degradation mechanism can be confirmed by blocking the terminal hydroxyl function for degradation studies (see below). For detailed mechanistic considerations, the degradation of $PEEP_{93}$ was evaluated. The formation of ethyl (2-hydroxyethyl) phosphate as predominant degradation product was confirmed by ^1H, ^{31}P NMR correlation spectroscopy as well as by diffusion ordered spectroscopy (DOSY) (Fig. 3).

Fig. 3 shows the overlay of ^{31}P DOSY NMR spectra, recorded at different time points within the degradation process of $PEEP_{93}$. While the diffusion coefficient of the triester signal (residual polymer) shifted to lower values upon increasing degradation time indicating decreasing molecular weight, the diffusion coefficient of the diester (degradation product) remained constant. This indicates the formation of a single degradation product with a constant molecular weight. Also, SEC overlay shows a gradual decrease of the molecular weight, and no random chain scission (cf. Fig. S15). In contrast, the ^{31}P DOSY NMR spectrum recorded within the degradation of PMEP showed polymeric degradation products with varying diffusion coefficients (Fig. S19), which results from branching points within the polymer structure. The release of one repeat unit as the main degradation product is further proven by the correlation of the signal of the methylene group adjacent to the terminal hydroxyl group in the ^1H NMR spectrum with the phosphorus diester signal in the ^{31}P NMR spectrum. This correlation can only occur when the terminal hydroxyl group is directly attached to a diester. Fig. 4 shows unambiguously that the methylene group adjacent to the terminal hydroxyl group correlates only with the diester, while no correlation with the triester was observed.

Furthermore, the HMBC spectrum clearly proves the backbiting of the terminal hydroxyl group by the correlation of two characteristic signals evolving in the ^1H and ^{31}P NMR respectively during the degradation process. During the degradation of $PEEP_{93}$ and $PMEP_{97}$, a characteristic signal at 18 ppm appears in the ^{31}P NMR spectra that can be attributed to the phosphorus atom located in the terminal five-membered cycle formed upon backbiting (Fig. 4). This signal correlates with a characteristic doublet appearing at 4.17 ppm (with J = 10.3 Hz) in the ^1H NMR spectra recorded during the degradation of both polymers and can be attributed to the methylene groups located in the terminal cycle. The integration of the signal in the phosphorus NMR remains almost constant during the whole degradation time indicating, that the number of terminal hydroxyl groups remained relatively constant upon degradation (a slight increase for $PEEP_{93}$ from ca. 1% to 3% was detected). This finding further contradicts a random ester cleavage along the polymer chain, which would lead to an increasing amount of end functionalities (see Fig. 5).

To understand the majority of the main-chain cleavage products, we performed density functional theory (DFT) calculations. A simplified model was adopted in the DFT calculations, in which the bulky polymer chain was replaced by a $C(CH_3)_3$ group, and only the first chain cleavage step was considered. As shown in Fig. 6(A), the main-chain cleavage products are ca. 4 kcal mol^{-1} thermodynamically more stable than the side-chain products for both polymers. It was assumed that the cleavage is preferred for the group along the same axis of the terminal oxygen atom in the structures of intermediate states (IMs, Fig. 6(B)) [21]. Therefore, we have computed the Gibbs free energies of such IMs for both polymers. The results show that the energy differences are negligible compared to the errors of DFT calculations, and there are no

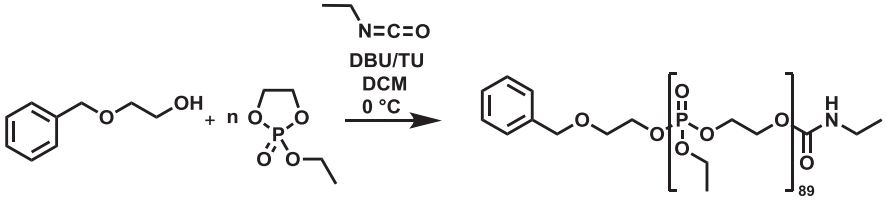

Scheme 3. Synthesis of end urethane-capped PEEP.

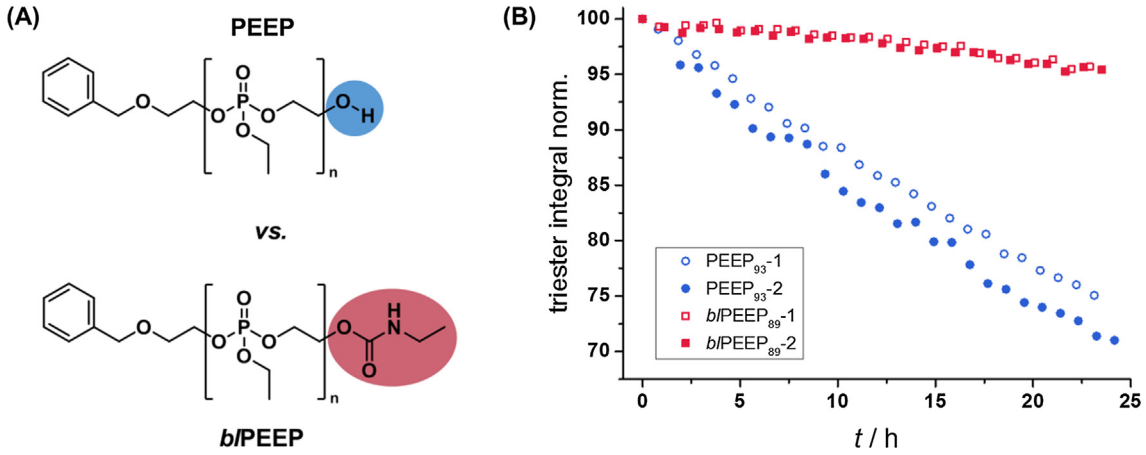

Fig. 7. (A) Chemical structures of PEEP with a terminal hydroxyl function and *bl*PEEP with terminal urethane. (B) Degradation profile of PEEP and *bl*PEEP derived from ^{31}P NMR spectra (two runs for each polymer are shown).

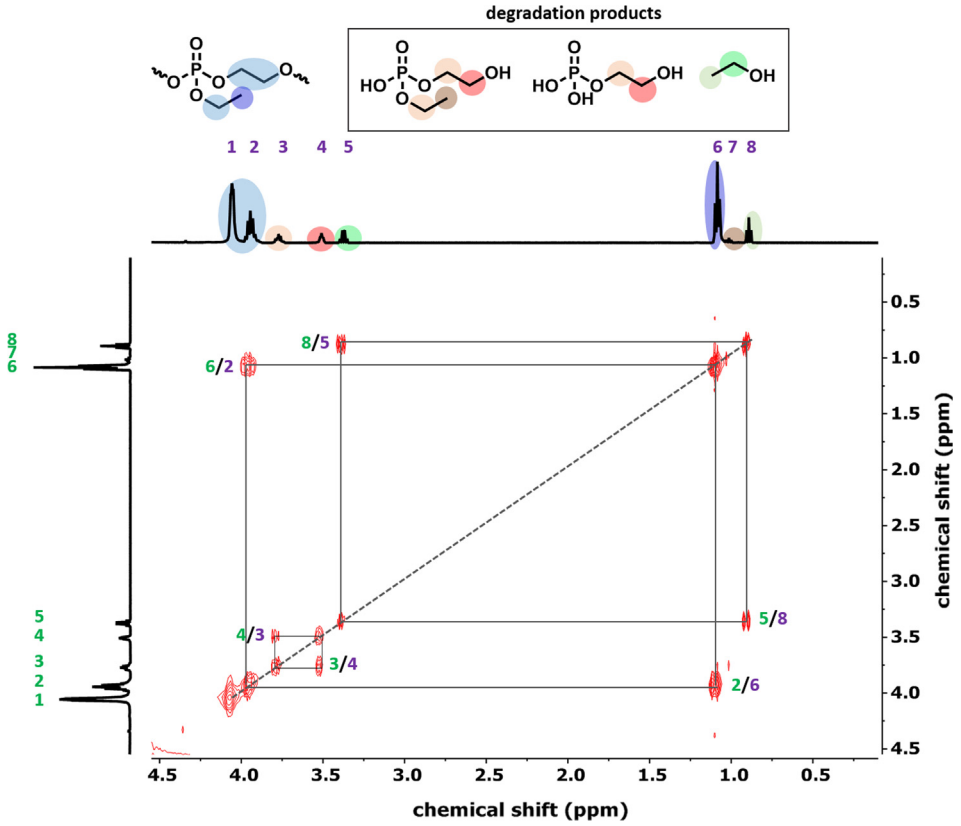

Fig. 8. 1H, 1H COSY NMR (500 MHz, 298 K, H2O/D2O (9:1)) of the degradation of PEEP with 1 M HCl containing 10% D2O. The NMR spectrum was recorded after 45 days of degradation.

energetic preferences between two IMs. Our DFT calculations therefore show that the main-chain cleavage are determined by the thermodynamics, rather than the kinetics.

In the case of poly(alkyl ethylene phosphate)s the backbiting and thus the formation of the 5-membered cyclic intermediate with a pentavalent P seems to be the major pathway for hydrolysis. We assume that by increasing the distance between the phosphates the nucleophilic attack of a terminal hydroxyl is reduced or that if no terminal hydroxyl is present (as for PPEs prepared by ADMET) the statistical hydrolysis of main- and side-chain occurs [31]. This also slows down the overall degradation and makes PPEs a very interesting material class with a broad spectrum of degradation times. Furthermore, in order to prove the catalytic role of the hydroxyl ions in the degradation process of polyphosphates, the polymer concentration was increased to 9.4 mg/mL (compared to 4.7 mg/mL in the above experiments). As the overall degradation kinetics are unchanged, we conclude that the hydroxyl ions are only involved catalytically during the basic hydrolysis (Fig. S14).

In order to further underline the crucial role of the terminal ethoxyhydroxy function in the degradation process of poly(alkyl ethylene phosphate)s, the terminal OH-group of PEEP was “blocked” by the reaction with ethyl isocyanate (Scheme 3). The “blocked PEEP” (*bl*PEEP) was prepared by terminating the AROP of EEP with an excess of ethyl isocyanate providing PEEP containing a urethane at the polymer chain end (Fig. S5 shows the ^{1}H NMR spectrum of the urethane-capped PEEP (blPEEP$_{89}$) proving a degree of end-capping of > 95%).

The degradation of *bl*PEEP$_{89}$ at pH 11 was analyzed by ^{31}P NMR spectroscopy analogously to the degradation of polymers with the terminal alcohol functionality and the degradation kinetics were compared (Fig. 7).

The degradation kinetics of the *bl*PEEP$_{89}$ proved to be significantly slower compared to PEEP-OH, supporting the suggested degradation mechanism by nucleophilic backbiting of the terminal alcohol group on the adjacent phosphotriester (Fig. 7). While for PEEP-OH within the first 20 h, ca 22–26% had been degraded, while for *bl*PEEP$_{89}$ only 4% cleavage of the phosphotriesters was observed. This slow degradation of *bl*PEEP$_{89}$ within the first 24 h could be attributed to either incomplete end functionalization or –more likely- degradation by the same backbiting mechanism as postulated above after a random ester had been cleaved along the polymer backbone. Such a random scission of ester linkages in the main-chain produces terminal alcohol functions, which can then induce degradation of the polymer by the suggested –and probably much faster-backbiting mechanism.

3.1. Acidic degradation

The degradation of PEEP$_{93}$ was also evaluated under acidic conditions at pH 0 using 1 M HCl containing 10% of D_2O. The degradation was observed in a timeframe of 45 days. Degradation studies under acidic conditions revealed a high stability of the PPEs in acidic media. Within the observed time, only 15% of the triester was cleaved (derived from ^{31}P NMR spectra (Fig. S8)). Furthermore, degradation of PEEP$_{93}$ under acidic conditions showed significantly higher release of ethanol compared to the degradation at pH 11 indicating an altered mechanisms under these conditions. Most likely, under acidic conditions the phosphoryl oxygen is protonated leading to an increased electrophilicity of the phosphorus atom. However, we still assume that the major degradation proceeding by backbiting of the terminal hydroxyl function since the ^{1}H, ^{1}H COSY NMR spectrum (Fig. 8) indicated 2-hydroxyethyl dihydrogen phosphate as the main degradation product, which might further be hydrolyzed to the monoester and ethanol.

4. Conclusion

In conclusion, we were able to prove that poly(alkyl ethylene phosphate)s undergo a backbiting hydrolysis under basic conditions resulting in the release of alkyl (2-hydroxyethyl) hydrogen phosphate as the main degradation product of the hydrolysis. The hydroxyl terminus of the polymers was found to play a crucial role in the degradation process, similar to the hydrolytic lability of RNA. Since degradation can be suppressed by chemical modification of the polymer terminus the selective introduction of hydroxyl functions in the polymer structure can be a useful tool for precise tailoring of the degradation characteristics of PPEs. Furthermore, both PEEPs showed enhanced stability as well as enhanced side chain release under acidic conditions indicating different degradation mechanisms for acidic and basic conditions. The findings for the synthetic PPEs might also be transferable to natural PPEs and opens the possibility to further tune their degradation behavior by chemical modification.

Acknowledgments

The authors thank the Deutsche Forschungsgemeinschaft (DFG WU750/6-1) for funding. The authors thank Angelika Manhart (MPIP) for synthetic assistance.

Data availability

Data will be made available on request.

Appendix A. Supplementary material

Supplementary data associated with this article can be found, in the online version, at https://doi.org/10.1016/j.eurpolymj.2018.08.058.

References

[1] B.D. Ulery, L.S. Nair, C.T. Laurencin, Biomedical applications of biodegradable polymers, J. Polym. Sci. Part B: Polym. Phys. 49 (12) (2011) 832–864.
[2] T. Haider, C. Völker, J. Kramm, K. Landfester, F.R. Wurm, Plastics of the future? The impact of biodegradable polymers on the environment and on society, Angew. Chem. Int. Ed. (2018), https://doi.org/10.1002/anie.201805766(ja).
[3] W. Amass, A. Amass, B. Tighe, A review of biodegradable polymers: uses, current developments in the synthesis and characterization of biodegradable polyesters, blends of biodegradable polymers and recent advances in biodegradation studies, Polym. Int. 47 (2) (1998) 89–144.
[4] Y.H. Lim, K.M. Tiemann, G.S. Heo, P.O. Wagers, Y.H. Rezenom, S. Zhang, F. Zhang, W.J. Youngs, D.A. Hunstad, K.L. Wooley, Preparation and in vitro antimicrobial activity of silver-bearing degradable polymeric nanoparticles of polyphosphoester-block-poly(l-lactide), ACS Nano 9 (2) (2015) 1995–2008.
[5] J. Zou, F. Zhang, S. Zhang, S.F. Pollack, M. Elsabahy, J. Fan, K.L. Wooley, Poly (ethylene oxide)-block-polyphosphoester-graft-paclitaxel conjugates with acid-labile linkages as a pH-sensitive and functional nanoscopic platform for paclitaxel delivery, Adv. Healthc. Mater. 3 (3) (2014) 441–448.
[6] O. Böstman, H. Pihlajamäki, Clinical biocompatibility of biodegradable orthopaedic implants for internal fixation: a review, Biomaterials 21 (24) (2000) 2615–2621.
[7] D.F. Williams, Mechanisms of biodegradation of implantable polymers, Clin. Mater. 10 (1) (1992) 9–12.
[8] S.J. Huang, M. Bitritto, K.W. Leong, J. Pavlisko, M. Roby, J.R. Knox, The Effects of Some Structural Variations on the Biodegradability of Step-Growth Polymers, Stabilization and Degradation of Polymers, American Chemical Society, 1978, pp. 205–214.
[9] S.K. Patra, R. Ahmed, G.R. Whittell, D.J. Lunn, E.L. Dunphy, M.A. Winnik, I. Manners, Cylindrical micelles of controlled length with a π-conjugated polythiophene core via crystallization-driven self-assembly, J. Am. Chem. Soc. 133 (23) (2011) 8842–8845.
[10] K.N. Bauer, H.T. Tee, M.M. Velencoso, F.R. Wurm, Main-chain poly(phosphoester)s: history, syntheses, degradation, bio-and flame-retardant applications, Prog. Polym. Sci. 73 (2017) 61–122.
[11] T. Steinbach, F.R. Wurm, Poly(phosphoester)s: a new platform for degradable polymers, Angew. Chem. Int. Ed. 54 (21) (2015) 6098–6108.
[12] J. Houseley, D. Tollervey, The many pathways of RNA degradation, Cell 136 (4) (2009) 763–776.
[13] C.L. Myers, R.G. Ireland, T.A. Garrett, E.D. Brown, Characterization of wall teichoic acid degradation by the bacteriophage ϕ29 appendage protein GP12 using synthetic substrate analogs, J. Biol. Chem. 290 (31) (2015) 19133–19145.
[14] K. Kawane, K. Motani, S. Nagata, DNA Degradation and Its Defects, Cold Spring Harb. Perspect. Biol. 6 (6) (2014).
[15] M.A. Kaczorowska, H.J. Cooper, Characterization of polyphosphoesters by Fourier transform ion cyclotron resonance mass spectrometry, J. Am. Soc. Mass Spectrom. Chem. 20 (12) (2009) 2238–2247.
[16] M.V. Chaubal, G. Su, E. Spicer, W. Dang, K.E. Branham, J.P. English, Z. Zhao, In vitro and in vivo degradation studies of a novel linear copolymer of lactide and ethylphosphate, J. Biomater. Sci. Polym. Ed. 14 (1) (2003) 45–61.
[17] H. Wang, L. Su, R. Li, S. Zhang, J. Fan, F. Zhang, T.P. Nguyen, K.L. Wooley, Polyphosphoramidates that undergo acid-triggered backbone degradation, ACS Macro Lett. 6 (3) (2017) 219–223.
[18] C. Wachiralarpphaithoon, Y. Iwasaki, K. Akiyoshi, Enzyme-degradable phosphorylcholine porous hydrogels cross-linked with polyphosphoesters for cell matrices, Biomaterials 28 (6) (2007) 984–993.
[19] T. Steinbach, G. Becker, A. Spiegel, T. Figueiredo, D. Russo, F.R. Wurm, Reversible bioconjugation: biodegradable poly(phosphate)-protein conjugates, Macromol. Biosci. 17 (2016) 1600377.
[20] T. Wolf, T. Steinbach, F.R. Wurm, A library of well-defined and water-soluble poly (alkyl phosphonate)s with adjustable hydrolysis, Macromolecules 48 (12) (2015) 3853–3863.
[21] J. Baran, S. Penczek, Hydrolysis of polyesters of phosphoric acid. 1. Kinetics and the pH profile, Macromolecules 28 (15) (1995) 5167–5176.
[22] B. Clément, B. Grignard, L. Koole, C. Jérôme, P. Lecomte, Metal-free strategies for the synthesis of functional and well-defined polyphosphoesters, Macromolecules 45 (11) (2012) 4476–4486.
[23] A.D. Becke, Density-functional thermochemistry. III. The role of exact exchange, J. Chem. Phys. 98 (7) (1993) 5648–5652.
[24] T. Clark, J. Chandrasekhar, G.W. Spitznagel, P.V. Schleyer, Efficient diffuse function-augmented basis sets for anion calculations. III. The 3–21 + G basis set for first-row elements, Li–F, J. Comput. Chem. 4 (3) (1983) 294–301.
[25] A.V. Marenich, C.J. Cramer, D.G. Truhlar, Universal solvation model based on solute electron density and on a continuum model of the solvent defined by the bulk dielectric constant and atomic surface tensions, J. Phys. Chem. B 113 (18) (2009) 6378–6396.
[26] G.W.T.M.J. Frisch, H.B. Schlegel, G.E. Scuseria, M.A. Robb, J.R. Cheeseman, G. Scalmani, V. Barone, B. Mennucci, G.A. Petersson, H. Nakatsuji, M. Caricato, X. Li, H.P. Hratchian, A.F. Izmaylov, J. Bloino, G. Zheng, J.L. Sonnenberg, M. Hada, M. Ehara, K. Toyota, R. Fukuda, J. Hasegawa, M. Ishida, T. Nakajima, Y. Honda,

O. Kitao, H. Nakai, T. Vreven, J.A. Montgomery Jr., J.E. Peralta, F. Ogliaro, M. Bearpark, J.J. Heyd, E. Brothers, K.N. Kudin, V.N. Staroverov, R. Kobayashi, J. Normand, K. Raghavachari, A. Rendell, J.C. Burant, S.S. Iyengar, J. Tomasi, M. Cossi, N. Rega, J.M. Millam, M. Klene, J.E. Knox, J.B. Cross, V. Bakken, C. Adamo, J. Jaramillo, R. Gomperts, R.E. Stratmann, O. Yazyev, A.J. Austin, R. Cammi, C. Pomelli, J.W. Ochterski, R.L. Martin, K. Morokuma, V.G. Zakrzewski, G.A. Voth, P. Salvador, J.J. Dannenberg, S. Dapprich, A.D. Daniels, Ö. Farkas, J.B. Foresman, J.V. Ortiz, J. Cioslowski, D.J. Fox, Gaussian 09, Revision D. 01, Gaussian, Inc., Wallingford CT, 2009.

[27] F. Zhang, J.A. Smolen, S. Zhang, R. Li, P.N. Shah, S. Cho, H. Wang, J.E. Raymond, C.L. Cannon, K.L. Wooley, Degradable polyphosphoester-based silver-loaded nanoparticles as therapeutics for bacterial lung infections, Nanoscale 7 (6) (2015) 2265–2270.

[28] S. Zhang, J. Zou, F. Zhang, M. Elsabahy, S.E. Felder, J. Zhu, D.J. Pochan, K.L. Wooley, Rapid and versatile construction of diverse and functional nanostructures derived from a polyphosphoester-based biomimetic block copolymer system, J. Am. Chem. Soc. 134 (44) (2012) 18467–18474.

[29] S. Schöttler, G. Becker, S. Winzen, T. Steinbach, K. Mohr, K. Landfester, V. Mailänder, F.R. Wurm, Protein adsorption is required for stealth effect of poly (ethylene glycol)- and poly(phosphoester)-coated nanocarriers, Nat. Nano 11 (4) (2016) 372–377.

[30] S. Zhang, H. Wang, Y. Shen, F. Zhang, K. Seetho, J. Zou, J.-S.A. Taylor, A.P. Dove, K.L. Wooley, A simple and efficient synthesis of an acid-labile polyphosphoramidate by organobase-catalyzed ring-opening polymerization and transformation to polyphosphoester ionomers by acid treatment, Macromolecules 46 (13) (2013) 5141–5149.

[31] G. Becker, L.-M. Ackermann, E. Schechtel, M. Klapper, W. Tremel, F.R. Wurm, Joining two natural motifs: catechol-containing poly(phosphoester)s, Biomacromolecules 18 (3) (2017) 767–777.

[32] I.E. Nifant'ev, A.V. Shlyakhtin, V.V. Bagrov, P.D. Komarov, M.A. Kosarev, A.N. Tavtorkin, M.E. Minyaev, V.A. Roznyatovsky, P.V. Ivchenko, Controlled ring-opening polymerisation of cyclic phosphates, phosphonates and phosphoramidates catalysed by heteroleptic BHT-alkoxy magnesium complexes, Polym. Chem. 8 (44) (2017) 6806–6816.

[33] S.J. de Jong, E.R. Arias, D.T.S. Rijkers, C.F. van Nostrum, J.J. Kettenes-van den Bosch, W.E. Hennink, New insights into the hydrolytic degradation of poly(lactic acid): participation of the alcohol terminus, Polymer 42 (7) (2001) 2795–2802.